J. Electroanal. Chem., 282 (1990) 239–252
Elsevier Sequoia S.A., Lausanne – Printed in The Netherlands

Polymer films on electrodes

Part 23. Ellipsometric study of the electrochemical redox processes of a thionine film on a glassy carbon electrode

Chongmok Lee, Juhyoun Kwak, Larry J. Kepley and Allen J. Bard

Department of Chemistry, The University of Texas, Austin, TX 78712 (U.S.A.)

(Received 6 January 1989; in revised form 8 November 1989)

ABSTRACT

Ellipsometry was used to observe the in situ electrochemical redox processes of a thionine film that was electrochemically deposited (thickness > 70 nm) on a glassy carbon electrode at 1.2 V from a 0.05 M H_2SO_4 solution containing 50 μM thionine. To determine the spatial distribution of the oxidized and reduced states during the reduction and oxidation of the film, the conversion process was simulated by a multilayer film model, where 8 or 9 discrete film layers were considered. Such simulations of the ellipsometric results show that the redox conversion of a thionine film proceeds from the electrode/film interface towards the solution and is controlled by electron hopping.

INTRODUCTION

This study concerns simultaneous ellipsometric and electrochemical measurements on an electrodeposited thionine film on a glassy carbon (GC) electrode. These measurements were used to determine how conversion of the film from the oxidized (O) to the reduced (R) state (or the reverse process) occurs in terms of the spatial distribution of O and R during the process. There have been several ellipsometric/electrochemical studies of polymer films: polyaniline [1], poly(vinylferrocene) [2], polymeric viologen [3], and polypyrrole [4]. Similar ellipsometry has been used to study the reduction process on metal oxide films [5,6].

Three modes of oxidative or reductive conversion of the film are usually considered [1,5,6], and these depend upon the rate of charge (electron and ion) propagation through the film, the experimental conditions of the potential application and the characteristic measurement or sampling time. (A) If the charge mobilities are high and the sampling time long, the conversion of the film appears spatially uniform, i.e., the O and R concentrations are not functions of the distance, x, into

0022-0728/90/$03.50

the film from the substrate surface. If the sampling time is sufficiently short, the O and R distributions during the conversion can be found for two limiting cases. (B) If electron mobility through the film is larger than ion mobility, conversion occurs from the film/solution interface towards the substrate electrode/film interface. (C) If ion mobility is larger than electron mobility, conversion proceeds from the electrode/film interface towards the film/solution interface. Previous studies [1,5,6] considered these alternatives and derived the ellipsometric behavior based on a two-layer model of the film. In the polyaniline study [1], spatially uniform conversion (case A) was found. In the work reported here, the conversion process was simulated by a multilayer film model (model D) [4,7–9], with up to 8 discrete film layers considered, and we have shown that the redox conversion of a thionine film proceeds from the electrode/film interface towards the solution. We have also studied redox conversion processes of a thionine film by chemical reduction and electrochemical oxidation.

EXPERIMENTAL

Experimental details about the optical cell, the ellipsometric apparatus, and the GC electrode have been described elsewhere [10]. Briefly, a Rudolph Research Model 2437 ellipsometer (Rudolph Research, Flander, NJ) equipped with a Model RR2000FT automatic rotating analyzer (5.4 rps) and interfaced to a Hewlett-Packard Model 9816S desk-top computer was employed. The characteristic sampling time for obtaining the ellipsometric parameters Ψ and Δ was changed depending upon how many sets of Fourier coefficients were averaged and whether the data were printed. The GC electrode was mounted in the bottom of a Teflon cell that contained auxiliary and reference electrodes and was polished to an optically flat condition before the deposition of thionine. The film deposition was accomplished by potentiostatic control of the GC electrode (area: 0.203 cm^2) at 1.20 V vs. a saturated calomel electrode (SCE) [11–13] or by cyclic potential sweeps between 1.30 and -0.15 V vs. SCE [14] in an aqueous solution containing ca. 50 μM thionine (Aldrich) in 0.05 or 0.5 M H_2SO_4 in the optical cell. Ellipsometric measurements on the redox conversion of the deposited films were performed after the solution containing monomer was replaced by an aqueous 0.05 or 0.5 M H_2SO_4 solution. Ellipsometric measurements of film growth during deposition and film conversion were made at a wavelength of 632.8 nm (He–Ne laser) and an angle of incidence of 67°. Titanium(III) chloride ($TiCl_3$, Aldrich) was employed as a reducing agent in experiments involving the chemical reduction of thionine monomer or the oxidized form of the thionine film [15]. An indium-doped SnO_2-coated glass (Delta Technologies, Stillwater, MN) electrode (working area, 1.2×1.2 cm) was also employed to observe the optical response (absorbance) during film conversion. The absorbance change of the film as a function of the applied potential was measured with an HP Model 8450 UV/VIS spectrophotometer (Hewlett-Packard, Palo Alto, CA) at 632 nm. The absorbance of a bare electrode in the same solution was used as a reference.

RESULTS AND DISCUSSION

Thionine film growth

Ellipsometry was employed to follow the electrochemical formation of a film by oxidation of thionine in 0.05 M H_2SO_4 containing 50 μM thionine deposited potentiostatically at +1.20 V on a GC substrate. Films were grown over a period of 22 h. Periodically the ellipsometric parameters Ψ and Δ were determined at +0.8 V vs. SCE (the oxidized state) and at −0.2 V vs. SCE (the reduced state); typical results are shown in Fig. 1 as circle symbols. Alternatively, films were grown by cyclic potential sweeps between −0.15 and +1.30 V vs. SCE in 0.5 M H_2SO_4 containing 50 μM thionine over a period of 4 h; typical ellipsometric results are also shown in Fig. 1 as triangle symbols; typical cyclic voltammograms for thionine deposition on GC are shown in Fig. 2 during cyclic potential sweep growth. Previous reports of film formation employed substrates of Pt, Au, and SnO_2 [12,14]. Among those substrates, SnO_2 was reported for deposition of the thickest thionine film, 12.7 nm [14]. The redox conversion process was not followed by ellipsometry

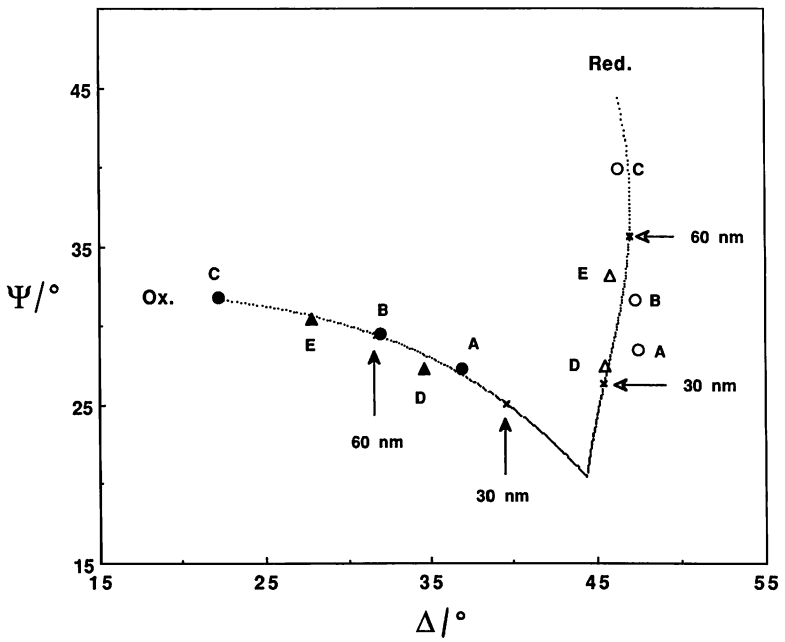

Fig. 1. Experimental and calculated ellipsometric data for the growth of a polymeric thionine layer on a GC electrode. Dotted lines are calculated with a uniform refractive index: $1.70-i(0.24)$ for the oxidized form and $1.66-i(0.03)$ for the reduced form. Symbol points show experimental ellipsometric data: (○, ●) potentiostatic growth (A, B, and C); (△, ▲) cyclic potential sweep growth (D and E); (●, ▲) oxidized form (at 0.8 V vs. SCE); (○, △) reduced form (at −0.2 V vs. SCE). (×) Calculations for every 30 nm thickness; pairs of equivalent points are labeled.

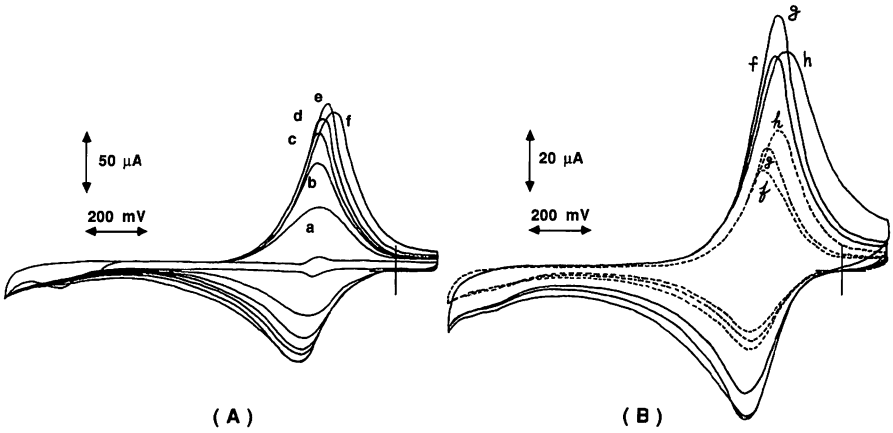

Fig. 2. Cyclic voltammograms for growth of a polymeric thionine layer on a GC electrode from a 50 μM thionine+0.5 M H_2SO_4 solution by cycling between 1.30 and −0.15 V vs. SCE. Curves a–h represent sequential scans. (A) Earlier part of film growth at a scan rate, v, of 100 mV/s. Small peaks in the middle represent monomeric thionine in solution. (B) Continuous film growth after (A) at v of 50 mV/s (———) or 20 mV/s (— — —).

because of the small film thickness. We chose GC as a substrate electrode because thicker layers of the polymeric film (> 70 nm) could be grown. The film thickness is a critical factor in examining redox conversion processes by ellipsometry.

The dotted curves in Fig. 1 represent our best fits with the thicknesses (d) and refractive indices (n) shown to the somewhat scattered experimental data, especially for the reduced film. We should note that the fit of n was not very precise. By using a larger real part and a smaller imaginary part of n, or vice versa, we could get almost the same fit. The ellipsometric growth curves can be fit moderately well up to a thickness of 80 nm by using n of $1.70 - i(0.24)$ for the oxidized form (n_O) and $1.66 - i(0.03)$ for the reduced form (n_R) at 632.8 nm. An n_O of $1.64 - i(0.24)$ and n_R of $1.50 - i(0.0)$ were previously reported [13,16] for a thinner film (< 5 nm) on a Pt substrate. If we tried to fit our data using these reported refractive indices, the growth curves showed a much large deviation from the data. Our growth curves in Fig. 1 are obtained using values for the imaginary part of n based on absorbance spectra in the visible region [13,16,17] even though determinations of n on very thin films are difficult [18].

In Fig. 2, cyclic voltammograms of thionine deposition on GC in monomer solution during repetitive sweeps are shown. During the early part of film deposition (Fig. 2A), the peak heights increased from an initial small peak for oxidation of monomeric thionine in solution, to wave (e) (scan rate, v, of 100 mV/s). After the time associated with wave (e), and at $v = 100$ mV/s, the v peak heights started to decrease and show some diffusive tailing (wave (f), Fig. 2A). If v was decreased to 50 or 20 mV/s (e.g., wave (f) in Fig. 2B), well-behaved surface waves of the deposited films were still observed. Previous reports indicate that the heights of the

characteristic thionine oxidation and reduction peaks increased to asymptotic limits after a certain number of cycles [14]. It is difficult to see the growth of the thionine film clearly by cyclic voltammetry; however, if we measured film status using ellipsometry, we could observe the film growth up to point E in Fig. 1. We attribute the slow growth of the thionine films to a slow charge transport rate in the films, because better-behaved surface waves are found at lower scan rates. These very slow growth kinetics may be a factor contributing to a film deposition which is not uniform in time.

Redox conversion in cyclic voltammetry

Previous reports [12,13,16] have shown that oxidation of thionine leads to a polymer of unknown structure that behaves as a collection of discrete units with redox properties similar to that of thionine monomer, namely [16]

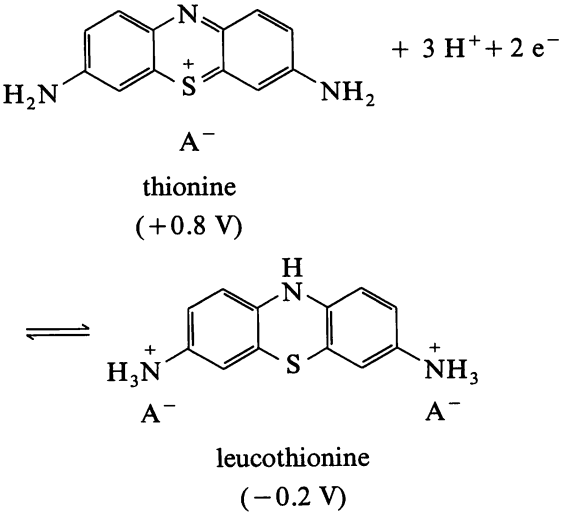

The interconversion between these states was studied with a film grown up to point E in Fig. 1 by both cyclic voltammetry (Fig. 3) and measurement of the ellipsometric parameters every 0.37 s (single set of Fourier coefficients, data storage) during cyclic potential sweeps between −0.15 and 0.8 V vs. SCE at scan rates, v, of 20, 50 and 100 mV/s in 0.5 M H_2SO_4 (Fig. 4). In Fig. 3, cyclic voltammograms of a deposited thionine film in a thionine-free solution are shown. In cyclic voltammetry of surface-confined redox species that show ideal thin layer behavior, the peak currents (i_p) are usually proportional to v and have a symmetrical shape [19]. However, for the thionine film at a v of 50 or 100 mV/s, the wave shapes resembled those of a redox couple in solution. In other words, slow charge transport through the polymer becomes the factor controlling the current at larger v. This has been seen with other polymer films at relatively slow scan rates, e.g., with plasma-polymerized vinylferrocene at low temperature (−70 °C) [20,21]. This charge transfer

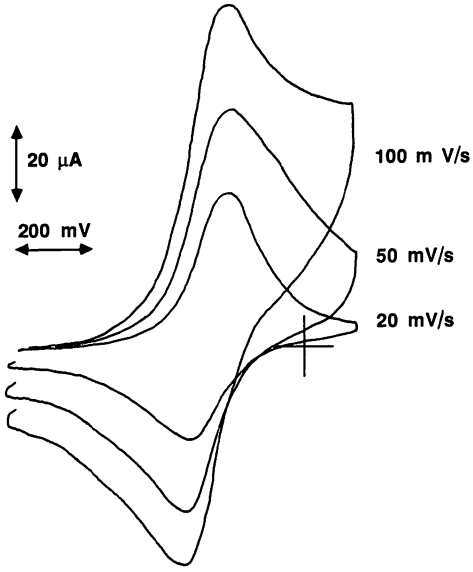

Fig. 3. Cyclic voltammetric waves of a thionine film deposited on a GC electrode in 0.5 M H_2SO_4 solution at v of 20, 50, and 100 mV/s (film grown to point E in Fig. 1).

rate effect is also found in ellipsometric experiments performed during the cyclic voltammetric scans (Fig. 4). As shown in Fig. 4, the redox conversion was not complete within the scan time at v of 50 and 100 mV/s, i.e., the O sites were not

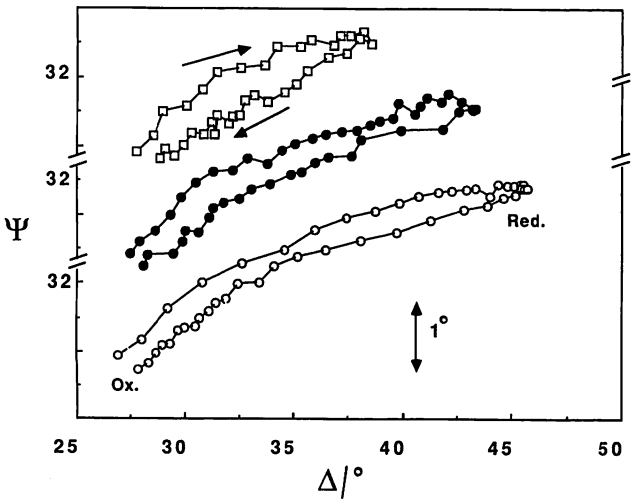

Fig. 4. Ellipsometric O/R conversion curves for a thionine layer (grown to point E in Fig. 1) by cyclic voltammetric scans between 0.8 and −0.2 V vs. SCE, obtained simultaneously with the Fig. 3 experiment. (○) 20 mV/s; (●) 50 mV/s; (□) 100 mV/s.

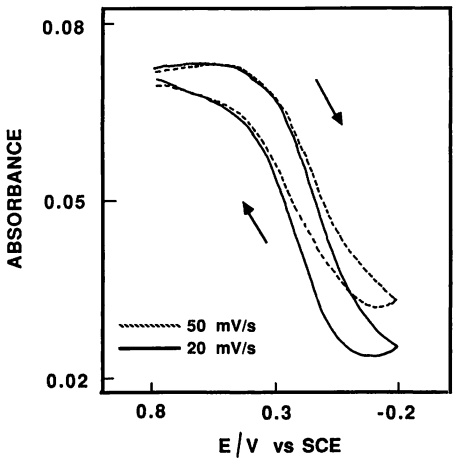

Fig. 5. Variation of absorbance of a film of thionine deposited on indium-doped tin oxide during potential sweeps between −0.2 and +0.8 V vs. SCE at 20 mV/s (———) and 50 mV/s (— — —) at a wavelength of 632 nm.

completely reduced to R, because the rate of charge transport was small compared to the experimental time scale [21]. However, for a thinner film, conversion was almost complete at $v = 50$ mV/s.

The electrochromic behavior of thionine films also indicates slow film conversion rates. The variation of the absorbance of a film deposited on a transparent indium-doped SnO_2-coated electrode [14] in 0.05 M H_2SO_4 solution was monitored at 632 nm during cyclic potential sweeps between −0.2 and 0.8 V vs. SCE. The data obtained at v of 20 and 50 mV/s are shown in Fig. 5. The absorbance of the fully oxidized state was 0.072. From the relations

$$A = \epsilon cd \tag{2a}$$

$$2.303\ \epsilon c = 4\pi k/\lambda \tag{2b}$$

(where A, d and k are the absorbance, film thickness, and imaginary part of the refractive index, respectively) the thickness of the oxidized state was estimated to be 35 nm, assuming that the imaginary part of n for the oxidized state, k_O, as measured above and in refs. 13 and 17, was about 0.24. In Fig. 5 we can see the incomplete redox conversion at v of 50 mV/s.

To check the film thickness an refractive index of the fully reduced film (equivalent to point E in Fig. 1), the ellipsometric parameters were measured at multiple angles of incidence (MAI), as shown in Fig. 6. In this experiment, to check effects of the cell components and surface imperfections, e.g., roughness, we measured ellipsometric parameters at 632.8 nm for the reduced thionine layer (similar to point E in Fig. 1) at multiple angles of incidence, MAI (Fig. 6). Each point represents the measured change in light of a range of angles of incidence, θ, from 61 to 71°; 2° steps were used. The moderately good fit of the data with the n_R

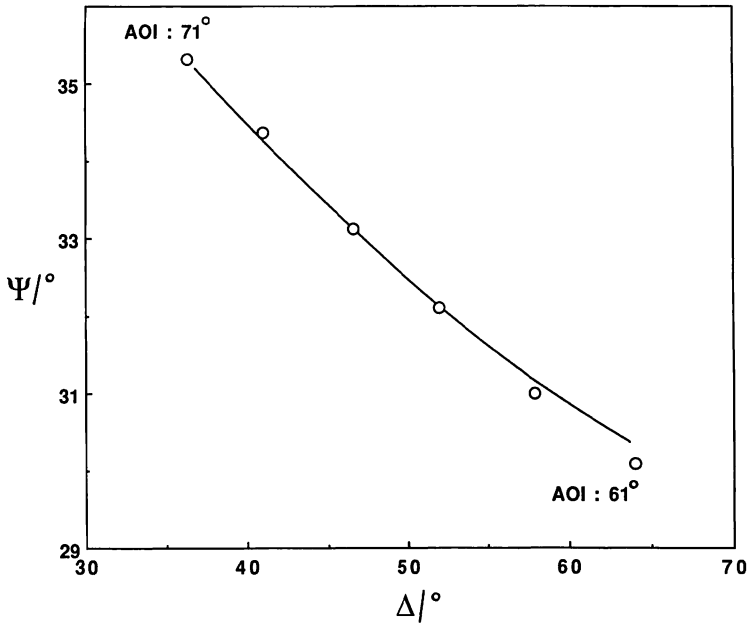

Fig. 6. Multiple angle of incidence data ($\theta = 61$–$71°$, in 2° steps) for a reduced thionine layer (thickness equivalent to point E in Fig. 1). The solid curve is a simulation of Ψ and Δ vs. θ for a 54.1 nm thick, isotropic layer ($n = 1.66 - i(0.03)$) on a GC electrode.

as found in the growth curves (Fig. 1) indicates that the surface roughness of this thionine film was sufficiently small to allow useful ellipsometric measurements. Moreover, to insure that the film brought to -0.2 V was completely reduced, for thicknesses at similar points to D and E in Fig. 1, a chemical reducing agent ($TiCl_3$) was added while monitoring the film by ellipsometry. During 15 min after addition of $TiCl_3$, no discernible change of the ellipsometric parameters was observed. Thus, there appear to be no unreduced thionine centers in the electrochemically reduced film.

Redox conversion in potential steps

Alternatively, conversion could be carried out with a potential step from an initial potential of 0.8 V to -0.2 V for 50 s, followed by a step back to 0.8 V, monitoring Ψ and Δ every 0.37 s (single set of Fourier coefficients and data storage) for a film grown to point C in Fig. 1, as shown in Fig. 7B.

An important advantage of thionine films for such conversion studies is the small effective diffusion coefficient for charge transport, D_E, of the order of 10^{-12} cm^2/s [11]. This makes the study of the conversion process possible with an ellipsometer with a relatively long sampling time (> 0.37 s) for a film thickness, d, ca. 50 nm, since the time for conversion is ca. d^2/D_E or ca. 25 s. Thus, as shown in Fig. 4, conversion can be monitored even at $v = 20$ mV/s. From Fig. 4 and similar studies,

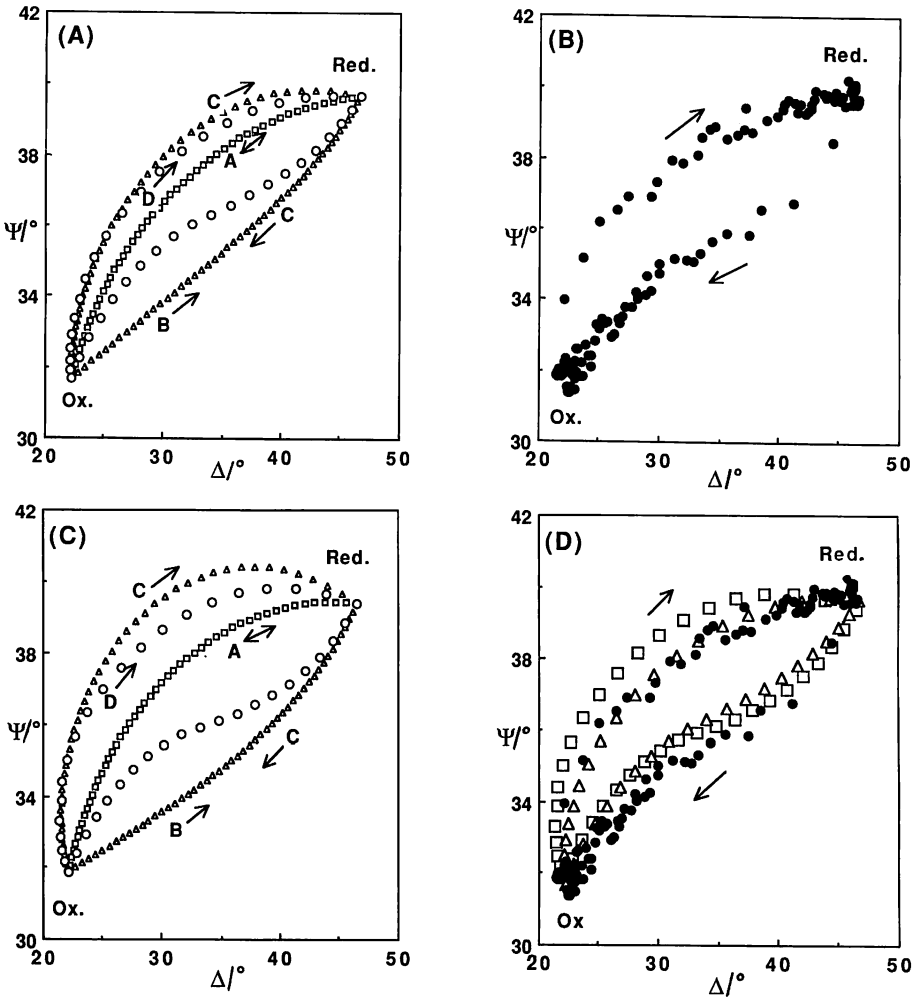

Fig. 7. Calculated and experimental ellipsometric conversion data for a thionine layer deposited on a GC electrode (thickness equivalent to point C in Fig. 1) in 0.05 M H_2SO_4, recorded at 632.8 nm at a 67° angle of incidence during potential steps (pulse width, 50 s) between 0.8 and −0.2 V vs. SCE. (A) Calculated with $n_O = 1.70 - i(0.24)$; $d_O = 81.0$ nm and $n_R = 1.65 - i(0.04)$; $d_R = 71.0$ nm. Calculated curves, A, B, C, and D correspond to the respective conversion models (see text): A (□); B and C (▲); D (○). (B) Experimental data. (C) Calculated with $n_O = 1.66 - i(0.25)$; $d_O = 91.0$ nm and n_R $1.55 - i(0.09)$; $d_R = 97.0$ nm. Labeling same as (A). (D) Overlap plot of experimental data with calculated multilayer conversion model D: experimental data (●); model D in (A) (△) model D in (C) (□).

we can deduce two phenomena. First, with the slower scan rate during cyclic potential sweeps, the ellipsometric curve showed a smaller degree of hysteresis for reduction as compared to oxidation. This implies that the lower the scan rate, the more the distribution of O and R at the electroactive sites inside the film are in equilibrium with the electrode potential [20]. Under these conditions, the ellipsomet-

ric data resemble that for a spatially uniform conversion (model A). Second, at higher scan rates, the redox conversion of the film during a sweep is incomplete, as discussed earlier. Thus, if we apply sufficiently low scan rates during the cyclic potential sweeps, the result of the ellipsometric curve will resemble that of the spatially uniform conversion, and R/O conversion will be complete. On the other hand, if we apply sufficiently fast scan rates, R/O conversion will be incomplete and the electroactive sites inside the film will not be in equilibrium with the electrode potential. We chose potential steps rather than the cyclic potential sweeps as the method of potential application for the simulation studies like our previous study [4].

Simulations

To determine the spatial distribution of O and R during the reduction and oxidation of the film, the refractive index change and thickness change must be incorporated in a simulation according to models A, B, or C. The refractive indices and thicknesses of pure O and R are those of the completely oxidized and reduced forms (n_O, n_R, and d_O, d_R) given earlier. Different simulated redox conversion curves were obtained for model A (uniform conversion), model B (from solution to substrate), and model C (from substrate to solution). In the latter two cases, the film was simulated by a two-layer model, as in previous cases [1,5,6] and also by a multilayer model, as shown schematically in Fig. 8. The following considerations hold for the different models. In the homogeneous film model (A), n and d are taken to vary uniformly with extent of conversion, f, where f = charge passed/total charge for complete conversion. For models B and C and a two-layer simulation, two homogeneous films with refractive indices n_O and n_R are assumed, with relative thicknesses a linear function of f and an orientation of the O and R layers determined by the model and the direction of reaction. For models A, B, and C, simulations were carried out for 50 steps, representing different stages of conversion, for each redox conversion process. For the multilayer model, 20 steps, indexed by i and representing different fractions of the film converted, were employed to represent the oxidation and 20 steps to represent the reduction. The Nernst diffusion layer approach [22] was used, where the thickness of the diffusion layer at different stages of the conversion was taken to be $i/10$ of the total film thickness ($i < 10$). This diffusion layer, at every stage, was divided into 8 or 9 discrete layers, indexed by j, and each of thickness d_{ij} and refractive index η_{ij}. The refractive index at each stage, i, in layer j was taken to be proportional to the fractional concentrations of O and R in layer j, $f_{O,ij}$ and $f_{R,ij}$, respectively, and the bulk refractive indices, n_O and n_R, i.e.,

$$n_{ij} = f_{O,ij} n_O + f_{R,ij} n_R \tag{3}$$

$$n_{ij} = f_{O,ij} n_O + (1 - f_{O,ij}) n_R \tag{4}$$

For example, for the step when O is converted to R, when the thickness of the diffusion layer was smaller than the thickness of the film (taken arbitrarily for $i = 1$

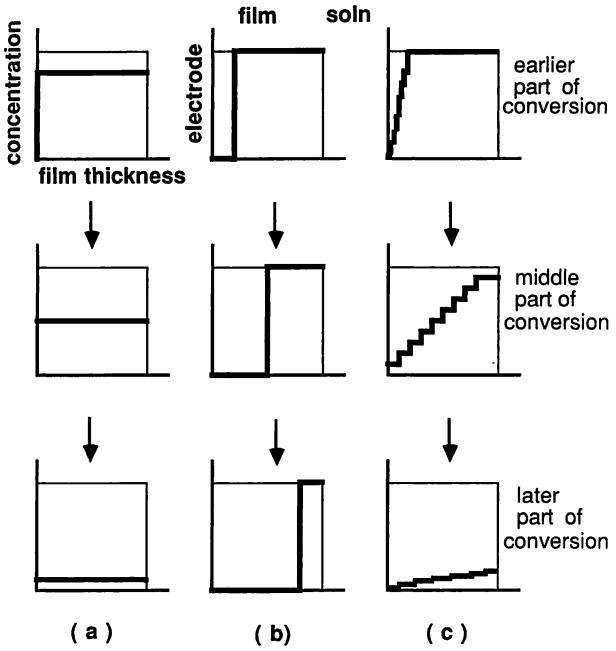

Fig. 8. Schematic diagram for the three conversion models: (a) homogeneous film conversion model (model A in text); (b) two-layer conversion model (from electrode/film toward film/solution; model C in text); (C) multilayer conversion model (model D in text).

to 9), the fractional concentration of the O state in the jth layer at the ith step was

$$f_{O,ij} = (2j-1)/16 \qquad (\text{for } j = 1 \text{ to } 8) \tag{5a}$$

$$f_{O,ij} = 1 \qquad (\text{for } j = 9) \tag{5b}$$

where the thickness of the jth layer at the ith stage was taken as

$$d_{ij} = f_{O,ij}(i/10)(d_O/8) + (1 - f_{O,ij})(i/10)(d_R/8) \qquad (\text{for } j = 1 \text{ to } 8) \tag{6a}$$

$$d_{ij} = [1 - (i/10)]\, d_O \qquad (j = 9) \tag{6b}$$

This adjustment of the simulation layer thickness with extent of oxidation was incorporated, because $d_O \neq d_R$ (see Fig. 7). When the thickness of the diffusion layer attained that of the film ($i = 10$ to 19), $f_{O,ij}$ was taken as

$$f_{O,ij} = [(2j-1)/16][1 - (i-10)/10] \qquad (j = 1 \text{ to } 8) \tag{7}$$

where the thickness of each jth layer is given by

$$d_{ij} = f_{O,ij}(d_O/8) + (1 - f_{O,ij})(d_R/8) \qquad (j = 1 \text{ to } 8) \tag{8}$$

This procedure allows simulation of the experimental results (Ψ and Δ) based on the approach used in ellipsometry for stratified planar isotropic structures [7] from

the refractive indices and film thicknesses of the completely oxidized and completely reduced forms (n_O, n_R, d_O, d_R) without any adjustable parameters. From the simulation results shown in Fig. 7A, the multilayer model (D) provided the best fit to the experimental ellipsometric curves among the above four models. In the redox process of Fig. 7, the experimental data of the earlier part of the conversion are closer to the two-film conversion model (C) among the three models A, B, and C, and those of the later part of the conversion are closer to the uniform film conversion model (A). Therefore, the multilayer model (D), which represents the production of a diffusion-limited concentration profile inside the film, is necessary to explain the diffusion-controlled conversion phenomenon.

We also tried to simulate the results with values for the real part of n reported previously [13,16], i.e., $n_O = 1.66 - i(0.25)$ and $n_R = 1.55 - i(0.09)$. While a moderately good fit for the growing film was obtained, the multilayer model (D) provided the better fit to the experimental data (Fig. 7C and D). Only the multilayer simulation can explain the subtle changes in curvature in the experimental curves, especially the oxidation curve, independent of the values of n_O and n_R used. Moreover, the absorbance data for monomeric leucothionine are not consistent with

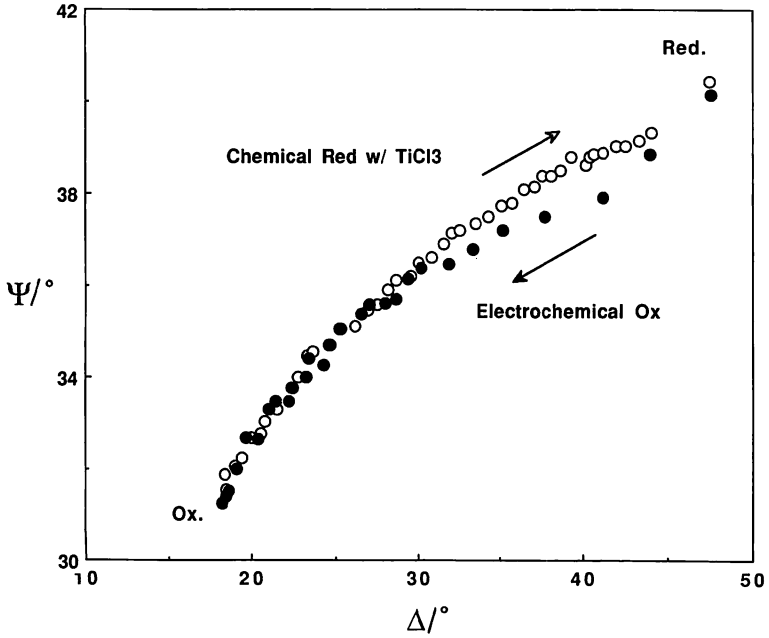

Fig. 9. Experimental ellipsometric conversion data of a thionine layer deposited on a GC electrode (equivalent to point C in Fig. 1 by CV growth) in 0.5 M H_2SO_4, recorded at 632.8 nm at a 67° angle of incidence. After holding the GC at +0.8 V vs. SCE, it was disconnected from the potentiostat. Oxidized film was reduced by adding $TiCl_3$ solution from the top of the cell (○). Chemically reduced film on GC was then reconnected to the potentiostat and oxidized at 0.8 V vs. SCE (●).

an n_R of $1.55 - i(0.09)$ for the film; the low absorbance at 632 nm would not predict such a large imaginary part. However, some absorbance at 632 nm of a deposited thionine film in the reduced state is possible. Alternatively, formation of a thin film on the GC surface upon oxidation [10,23] may make a very small contribution to the ellipsometric measurement.

Although this multilayer model used a simple Nernst diffusion layer model to determine the concentration profile with 8 or 9 discrete layers rather than a more rigorous simulation of the concentration profiles, the results are in good agreement with the experimental data, so that this approach appears adequate for this system.

Ellipsometry with chemical reduction of film

As a final test of our model for electrochemical film oxidation and reduction, we carried out an experiment with chemical reduction of the film by Ti(III) in solution. In this case conversion (O to R) must occur from the film/solution interface (as opposed to the electrochemical reduction case), since both electrons' compensating ions are supplied from the solution. Results are shown in Fig. 9. The GC, coated with a film equivalent to point C of Fig. 1, was first held at +0.8 V for 5 min to oxidize the thionine film. The GC was disconnected from the potentiostat and ellipsometric data were taken as a $TiCl_3 + H_2SO_4$ solution was added through the top of the cell, yielding the open circles in Fig. 9. The GC was reconnected and a potential of +0.8 V was applied, yielding the closed circles in Fig. 9. These results can be compared to those in Fig. 7B, where the reduction was carried out electrochemically. Note in particular the much smaller amount of hysteresis in the curves in Fig. 9. The results appear to be at least qualitatively consistent with model B for reduction and model C for oxidation (see Fig. 7A).

CONCLUSIONS

This ellipsometric study of the modes of spatial propagation of oxidized and reduced sites inside a thionine film during a diffusion-limited electrochemical redox conversion process suggests that the direction of this process is from the electrode/film interface towards the film/solution interface. This conversion direction is consistent with electron transfer (rather than ion transport) being the rate-limiting process [18]. Note, however, that a previous study of the surface-enhanced Raman spectroscopy of a thionine film [12] reported the reverse direction of the conversion process for a film consisting of less than 15 monolayers of thionine on a gold electrode.

ACKNOWLEDGEMENT

The support of this research by the National Science Foundation (CHE8901450)and the Robert A. Welch Foundation is gratefully acknowledged.

REFERENCES

1 S. Gottesfeld, A. Redondo and S.W. Feldberg, J. Electrochem. Soc., 134 (1987) 272.
2 C.M. Carlin, L.J. Kepley and A.J. Bard, J. Electrochem. Soc., 132 (1985) 353; G.C. Winston and C.M. Carlin, ibid., 135 (1988) 789.
3 L.J. Kepley and A.J. Bard, in preparation.
4 C. Lee, J. Kwak and A.J. Bard, J. Electrochem. Soc., 136 (1989) 3720.
5 M.A. Hopper and J.L. Ord, J. Electrochem. Soc., 120 (1973) 183.
6 J.C. Clayton and D.J. DeSmet, J. Electrochem. Soc., 123 (1976) 174.
7 R.M.A. Azzam and N.M. Bashara, Ellipsometry and Polarized Light, North Holland, Amsterdam, 1977.
8 R.H. Muller and C.G. Smith, Surf. Sci., 56 (1976) 440.
9 G.E. Jellison, Jr. and F.A. Modine, J. Opt. Soc. Am., 72 (1982) 1253.
10 L.J. Kepley and A.J. Bard, Anal. Chem., 60 (1988) 1459.
11 W.J. Albery, M.G. Boutelle, P.J. Colby and A.R. Hillman, J. Electroanal. Chem., 133 (1982) 135.
12 K. Hutchinson, R.E. Hester, W.J. Albery and A.R. Hillman, J. Chem. Soc. Faraday Trans. 1, 80 (1984) 2053.
13 A. Hamnett and A.R. Hillman, J. Electroanal. Chem., 233 (1987) 125.
14 T.I. Quickenden and I.R. Harrison, J. Electrochem. Soc., 132 (1985) 81.
15 L. Michaelis, M.P. Schubert and S. Granick, J. Am. Chem. Soc., 62 (1940) 204.
16 A. Hamnett and A.R. Hillman, Ber. Bunsenges. Phys. Chem., 91 (1987) 329.
17 A. Hamnett and A.R. Hillman, J. Electrochem. Soc., 244 (1988) 353.
18 S. Gottesfeld in A.J. Bard (Ed.), Electroanalytical Chemistry, Vol. 15, Marcel Dekker, New York, 1988, pp. 182–187.
19 R.F. Lane and A.T. Hubbard, J. Phys. Chem., 77 (1973) 1401.
20 P. Daum, J.R. Lenhard, D. Rolison and R.W. Murray, J. Am. Chem. Soc., 102 (1980) 4649.
21 R.W. Murray in A.J. Bard (Ed.), Electroanalytical Chemistry, Vol. 13, Marcel Dekker, New York, 1984, pp. 200–206.
22 A.J. Bard and L.R. Faulkner, Electrochemical Methods: Fundamentals and Applications, Wiley, New York, 1980, Ch. 1.
23 R.C. Engstrom, Anal. Chem., 54 (1982) 2310.